Template iterations of quadratic maps and hybrid Mandelbrot sets

Anca Rădulescu*,[1], Brandee Williams[1]
[1] Department of Mathematics, SUNY New Paltz, NY 12561

arXiv:1609.03949v1 [math.DS] 13 Sep 2016

Abstract

We continue previous work in template iterations of pairs of quadratic complex maps. As a particular problem within the field of non-autonomous discrete systems, we consider iterations of two quadratic maps $f_{c_0} = z^2 + c_0$ and $f_{c_1} = z^2 + c_1$, according to a prescribed binary sequence, which we call *template*. We study the asymptotic behavior of the critical orbit, and define the Mandelbrot set as the locus for which this orbit is bounded. However, unlike in the case of single maps, this concept can be understood in several ways. For a fixed template, one may consider this locus as a subset of the parameter space $(c_0, c_1) \in \mathbb{C}^2$; for fixed quadratic parameters, one may consider the set of templates which render a bounded critical orbit. In this paper, we consider both situations, as well as *hybrid* combinations of them, and study basic topological properties of these sets.

1 Introduction

The family of logistic maps has been over the years one of the most studied examples in the theory of discrete dynamical systems. In the context of complex functions $f_c \colon \mathbb{C} \to \mathbb{C},\ f_c(z) = z^2 + c$, for $c \in \mathbb{C}$, results going all the way back to the original theory of Fatou and Julia describe thoroughly the behavior of the orbits in the dynamic complex plane, as well as in the parameter plane.

The prisoner set of a complex map f is defined as the set of all points in the dynamic plane, whose orbits are bounded. The escape set of a complex map is the set of all points whose orbits are unbounded. We call the Julia set of f their common boundary $J(f)$. We call the filled Julia set, the union of prisoner points with their boundary $J(f)$.

For polynomial maps, it has been shown that the connectivity of a map's Julia set is tightly related to the structure of its critical orbits (i.e., the orbits of the map's critical points). Due to extensive work spanning almost one century, from Julia [9] and Fatou [10] until recent developments [1, 12], we now have the following result, known as

The Fatou-Julia Theorem. *For a polynomial with at least one critical orbit unbounded, the Julia set is totally disconnected if and only if all the bounded critical orbits are aperiodic.*

For iterations of a single quadratic map [2, 6], the Fatou-Julia Theorem implies that the Julia set is either totally connected, for values of c in the Mandelbrot set (i.e., if the orbit of the critical point 0 is bounded), or totally disconnected, for values of c outside of the Mandelbrot set (i.e., if the orbit of the critical point 0 is unbounded).

In nature, however, it is unlikely that systems evolve according to the same identical dynamics along time. A more realistic mathematical framework to model the variability and errors that appear replication systems is to consider time-dependent (non-autonomous) iterations, in which the iterated map may change between steps (evolve in time).

Random iterations have been studied since the early 1990's, starting with the pioneering work of Fornaess and Sibony [7]. In the case of simply alternating two quadratic maps, Danca et al. have showed that the Julia set can be disconnected without being totally disconnected [5]. They further related this extension to the Fatou-Julia theorem for complex polynomials of degree four,

[1]Assistant Professor, Department of Mathematics, State University of New York at New Paltz; New York, USA; Phone: (845) 257-3532; Email: radulesa@newpaltz.edu

and showed that alternated Julia sets exhibit graphical alternation. More recent work has been further addressing dynamic of the system and topological properties of the Julia and Mandelbrot set in the context of non-autonomous iterations [4, 3, 14].

In previous work [13], the authors have considered the iteration process of two different functions, f_{c_0} and f_{c_1}, according to a general binary symbolic sequence (which we called a *template*), in which the zero positions correspond to iterating the function f_{c_0} and the one positions correspond to iterating the function f_{c_1} . We view template iterations as a more appropriate framework for replication or learning algorithms that appear in nature, with patterns that evolve in time, and which may involve occasional, random or periodic "errors." While our results generally agree with existing results in non-autonomous iterations, our interest resides more specifically in understanding the dependence of the dynamic behavior on the two primary features of this system's hardwiring: (1) the complex parameter pair (c_0, c_1) that fixes the iterated maps and (2) the structure of the template, i.e. the particular succession (timing) of the 0s and 1s that govern the iteration order.

1.1 The quadratic family and template iterations

We will be working within the complex quadratic family

$$\{f_c \colon \mathbb{C} \to \mathbb{C} \ / \ f_c(z) = z^2 + c, \text{ with } c \in \mathbb{C}\}$$

For fixed parameters $c_0, c_1 \in \mathbb{C}$, and a fixed binary sequence $\mathbf{s} = (s_n)_{n\geq 0} \in \{0,1\}^\infty$, one can define the template orbit for any $z_0 \in \mathbb{C}$ as the sequence $o_{\mathbf{s}}(z_0) = (\xi_n)_{n\geq 0}$ constructed recursively, for every $n \geq 0$, as:

$$\xi_{n+1} = f_{c_{s_n}}(\xi_n)$$

In previous work, we considered the extension of the traditional Mandelbrot set for a symbolic template system. Since, in order to construct a template Julia set, we need both a complex parameter pair (c_0, c_1) and a symbolic template, we can consider objects in two different parameter spaces: in $\mathbb{C}^2$ (for a fixed template $\mathbf{s}$) and $\{0,1\}^\infty$ (for a fixed pair (c_0, c_1)). We defined two main types of "Mandelbrot" sets, as follows:

Definition 1.1. *Fix $\mathbf{s} \in \{0,1\}^\infty$ a symbolic sequence. The corresponding **fixed-template Mandelbrot set** is defined as:*

$$\mathcal{M}_{\mathbf{s}} = \{(c_0, c_1) \in \mathbb{C}^2, \text{ where } o_{\mathbf{s}}(0) \text{ is bounded } \}$$

Definition 1.2. *Fix $(c_0, c_1) \in \mathbb{C}^2$. The corresponding **fixed-map Mandelbrot set** is defined as:*

$$\mathcal{M}_{\mathbf{c_0},\mathbf{c_1}} = \{\mathbf{s} \in \{0,1\}^\infty, \text{ where } o_{\mathbf{s}}(0) \text{ is bounded } \}$$

We may consider each template $\mathbf{s} \in \{0,1\}^\infty$ as corresponding to the binary expansion of a number $a_{\mathbf{s}} \in [0,1]$. Then a fixed-map Mandelbrot set $\mathcal{M}_{\mathbf{c_0},\mathbf{c_1}}$ can be viewed as the subset of all $a_{\mathbf{s}} \in [0,1]$ for which the template orbit $o_{\mathbf{s}}(0)$ under (c_0, c_1) is bounded. We can then define a mixed, or *hybrid* Mandelbrot set, potentially related to phenomena of averaging out chaos, as described in non-autonomous iterations literature.

Definition 1.3. *Fix $c_0 \in \mathbb{C}$. The corresponding **hybrid Mandelbrot set** is defined as:*

$$\mathcal{M}_{\mathbf{c_0}} = \{(c_1, b) \in \mathbb{C} \times [0,1], \text{ with } b = \mathcal{L}(\mathcal{M}_{\mathbf{c_0},\mathbf{c_1}})\}$$

where $\mathcal{L}$ designates the Lebesgue measure on the interval $[0,1]$.

The main goal of this paper is to visualize and study the structure of these sets, in particular understand their dependence on the complex parameters and on the template structure, whichever appropriate in each case.

1.2 Escape radius for template iterations

It is an established result [15] (which we reproduce here for the sake of completion) that iterations of single quadratic complex maps exhibit the escape radius $R_e = 2$. More precisely:

Theorem 1.4. *In the case of single quadratic map iterations: For any value of the parameter c, the critical orbit (z_n) (for $z_0 = 0$) under the function $f_c(z) = z^2 + c$ has the escape radius $r = 2$. That is, if $|z_N| > 2$ for some positive integer N, then $|z_n| > 2$ for all $n \geq N$, and $|z_n| \nearrow \infty$ as $n > N$.*

More abstract results have been formulated by Comerford et al. for the case of random iterations [4]. As per the reference, suppose we take $d \geq 2$, $K \geq 1$, $M \geq 0$ and let $(P_m)_{m=1}^{\infty}$ be a bounded sequence of polynomials, that is: (1) the degree d_m of each P_m satisfies $2 \leq d_m \leq d$; (2) the leading coefficients a_m satisfy $1/K \leq a_m \leq K$; (3) all coefficients of all P_m are within th disc of radius M. Then there exists $R > 0$ (called escape radius for the sequence of P_m) such that: for all $m \geq 0$ and all $|z| \geq R$, we have $|P_n \circ \ldots \circ P_{m+2} \circ P_{m+1}(z)| \to \infty$ as $n \to \infty$. Comerford et al. [4] show that one can find an escape radius R which depends only on the bounds d, K and M and works for every sequence which satisfies these bounds.

In our particular setup, we aim to show that in particular cases of template iterations, the escape radius remains $R_e = 2$. This will be extremely useful for our investigation, especially when numerically computing and illustrating fixed map and hybrid Mandelbrot sets, allowing us a computer assisted approach to Mandelbrot slices. The value does not hold, however, for arbitrary template iterations. Consider, for example, a value of c_0 outside of the traditional Mandelbrot set. According to Theorem 1.4, the orbit of zero will leave the disk of radius $R_e = 2$ after a certain number of iterations of f_{c_0}, and never return: $0 \to z_1 \to z_2 \to \ldots z_N$, with $|z_N| > 2$. Consider now a point z' in the filled Julia set of f_{c_0}, and choose $c_1 = z' - z_N^2$. Choose the template $\mathbf{s}$ to be zero everywhere, except on the $N + 1^{th}$ position. Then the orbit $o_{\mathbf{s}}(0)$ leaves the escape disk in N iterates (since $|z_N| > 2$), but $z_{N+1} = z_N^2 + c_1 = z'$, and the orbit remains henceforth bounded (all future iterations are under f_{c_0}). While this is a valid counterexample, it not robust, since the filled Julia set is Fatou dust for a c_0 outside of the Mandelbrot set, hence the choice of z', and subsequently c_1, is made from a set of area zero.

For arbitrary $(c_0, c_1) \in \mathbb{C}$, call, as before, $o_{\mathbf{s}}(0) = (\xi_n)_n$. Similarly to the traditional case, we can prove the folowing lemma.

Lemma 1.5. *Suppose $|\xi_N| > \max\{2, |c_0|, |c_1|\}$ for some N. Then $|\xi_n| > 2$ for all $n \geq N$, and $|\xi_n| \nearrow \infty$ as $n > N$.*

Proof of lemma. Suppose $|\xi_n| > 2$ for some $n \geq N$ and calculate:

$$\frac{|\xi_{n+1}|}{|\xi_n|} = \frac{|f_{c_{s_n}}(\xi_n)|}{|\xi_n|} = \frac{|z\xi_n^2 + c_{s_n}|}{|\xi_n|} \geq \frac{|\xi_n|^2 - |c_{s_n}|}{|z\xi_n|} = |\xi_n| - \frac{|c_{s_n}|}{|\xi_n|}$$

Since $|\xi_n| > |c_{s_n}|$ for all n, the right side $|z_n| - \frac{|c_1|}{|z_n|} > |z_n| - 1$. Since $|\xi_n| > 2$, we further have:

$$\frac{|\xi_{n+1}|}{|\xi_n|} > |\xi_n| - 1 > 1$$

Since $|\xi_N| > 2$, this implies by induction that $|\xi_n| > 2$ for all $n \geq N$. In addition, we have $|\xi_{n+1}| > |\xi_n|$ for $n \geq N$, implying that the orbit converges in radius to the its upper bound. If we assume that this upper bound is a finite number $l = \lim_{n\to\infty} |\xi_n|$, we get, taking limit on both sides of

$\frac{|\xi_{n+1}|}{|\xi_n|} \geq |\xi_n| - 1$, that the limit $l \leq 2$, contradiction with the fact that l is the upper bound for a sequence of values larger than 2. It follows that the limit $\lim_{n\to\infty} |\xi_n| = \infty$.

□

We prove below that $r = 2$ still works as the escape radius for template iterations if we assume $c_0 = 0$, ot if we assume $2 > \max\{|c_0|, |c_1|\}$.

Theorem 1.6. *For fixed $c_0 = 0$ and any value of the parameter $c_1 \in \mathbb{C}$, the template orbit (ξ_n) of $\xi_0 = 0$ under $(0, c_1)$ has escape radius $r = 2$. That is, if $|\xi_N| > 2$ for some positive integer N, then $|\xi_n| > 2$ for all $n \geq N$, and $|\xi_n| \nearrow \infty$ as $n > N$.*

Proof. Suppose first that we are in the case $|c_1| \leq 2$. From $|\xi_N| > 2$, it follows automatically in this case that $|\xi_N| > \max\{2, |c_0|, |c_1|\}$. The hypothesis of the Lemma 1.5 holds, implying that $|\xi_n| > 2$ for all $n \geq N$, and $|\xi_n| \nearrow \infty$ as $n > N$.

We have to analyze now the case $|c_1| > 2$. We aim to track down when the critical orbit $o_{s_n}(0)$ leaves the disk of radius 2. The orbit will remain zero as long as the map f_{c_0} is iterated (throughout the first batch of zeros in the template). If f_{c_1} is never iterated, the critical orbit is trivial. Otherwise, the first nonzero orbit entry will be $\xi_N = f_{c_1}(0) = c_1$, with $|\xi_N| > 2$. This will be squared repeatedly over the next batch of zero template entries. If all the remaining template entries are zero, the orbit will be, for all $n \geq 0$, $\xi_{N+n} = c_1^{2^n}$, with $|\xi_{N+n}| > 2$. If there is at least one additional nonzero entry in the template, at position $N + K$, then $\xi_{N+K} = c_1^{2^K}$, and $\xi_{N+K+1} = c_1^{2^{K+1}} + c_1$. Notice that $|\xi_{N+K+1}| = |c_1^{2^{K+1}} + c_1| = |c_1|(|c_1|^{2^{K+1}-1} - 1) > |c_1| > 2$. Hence ξ_{N+K+1} satisfies the conditions of Lemma 1.5 and the orbit escapes. In either case, once the orbit escapes the disk of radius $r = 2$, it continues to increase to ∞.

□

Theorem 1.7. *For $(c_0, c_1) \in \mathbb{C}^2$ with $|c_0|, |c_1| \leq 2$, the template orbit (ξ_n) of $\xi_0 = 0$ under (c_0, c_1) has escape radius $R_e = 2$.*

Proof. Follows directly from Lemma 1.5.

□

2 Structure of fixed-map Mandelbrot sets

In this section, we will study the structure of fixed map Mandelbrot sets, for different pairs (c_0, c_1). Throughout the section, we want to insure we work with values of c_0 and c_1 for which the escape radius $R_e = 2$ holds (see previous section). To fix our ideas, we will work with parameter values within the disc of radius $R_e = 2$ ($c_0, c_1 \in \mathbb{D}(2)$), which satisfy the escape radius property.

Since later in the paper we perform a computer-assisted numerical analysis, we will use truncated templates in order to illustrate our sets. We therefore find it useful to define finitely iterated versions of our sets (that is, for binary templates of finite length N), and explore the limit behavior as $N \to \infty$.

Definition 2.1. *We call an N-root a finite binary sequence $\langle \mathbf{s} \rangle = s_1 \dots s_N$. We will use the notation $\{0,1\}^N$ for the set of all N-roots. We say that two templates $\mathbf{s}$ and $\mathbf{s}' \in \{0,1\}^\infty$ have a common N-root if they agree up to the Nth position: $s_j = s'_j$, for $1 \leq j \leq N$.*

Note. In the interest of making our terminology most convenient for our purposes, we do not require of N to be maximal, hence the common root of two templates is not uniquely defined.

Definition 2.2. *We will use the notation $o_{\langle \mathbf{s} \rangle}(\xi_0)$ for the finite orbit of a point ξ_0 under the N-root $\langle \mathbf{s} \rangle$. We will also use $o^j_{\mathbf{s}}(\xi_0)$ and $o^j_{\langle \mathbf{s} \rangle}(\xi_0)$ to designate specifically the j-th iterate of ξ_0 under an infinite template $\mathbf{s}$ and respectively under an N-root $\langle \mathbf{s} \rangle$.*

Definition 2.3. *For a fixed pair $(c_0, c_1) \in \mathbb{C}^2$, the N-**rooted fixed-map Mandelbrot set** is defined as:*

$$\mathcal{M}^N_{\mathbf{c_0},\mathbf{c_1}} = \{\mathbf{s} \in \{0,1\}^\infty, \text{ with } |o^N_{\mathbf{s}}(0)| < R_e\}$$

With these definitions, the following lemma is trivial:

Lemma 2.4. *For any (c_0, c_1) that satisfy the escape radius and any arbitrary integer $N \geq 1$ we have that $\mathcal{M}^{N+1}_{c_0,c_1} \subset \mathcal{M}^N_{c_0,c_1} \subset \mathcal{M}_{c_0,c_1}$.*

Proof. Suppose $\langle \mathbf{s} \rangle$ is an N-root such that $|o^N_{\langle \mathbf{s} \rangle}(0)| > R_e$ (that is, the orbit of $\xi_0 = 0$ escapes by the time iteration reaches the end of the N-root). Then none of the templates $\mathbf{s} \in \{0,1\}^\infty$ with the common N-root $\langle s \rangle$ are in $\mathcal{M}_{\mathbf{c_0},\mathbf{c_1}}$.

In order to put a structure (e.g., order) on the set of templates, and more easily represent them when discussing fixed-map Mandelbrot sets, we will identify them with binary expansions of real numbers in the unit interval. Consider the map:

$$\psi \colon \{0,1\}^\infty \to [0,1]$$

$$\psi(\mathbf{s}) = \sum_{n=1}^{\infty} s_n 2^{-n} \text{ for all } \mathbf{s} = s_1, s_2, \ldots$$

We will illustrate and study the sets $\mathcal{M}_{c_0,c_1}$ and $\mathcal{M}^N_{c_0,c_1}$ as their representations in $[0,1]$, provided by the images $\psi(\mathcal{M}_{c_0,c_1})$ and $\psi(\mathcal{M}^N_{c_0,c_1})$.

Remark. Notice that ψ is surjective, but not injective. In other words: while any number in $[0,1]$ has at least one binary expansion, some numbers do have multiple expansions – a finite one, and an infinite one (e.g., $0.1 = 0.0\overline{1}$).

Theorem 2.5. *For every (c_0, c_1) satisfying the escape radius condition, $\mathcal{M}^N_{c_0,c_1}$ is a nested sequence of sets with*

$$\bigcap_{N=1}^{\infty} \mathcal{M}^N_{c_0,c_1} = \mathcal{M}_{c_0,c_1}$$

Proof. Recall that $\mathcal{M}_{c_0,c_1} \subset \mathcal{M}^{N+1}_{c_0,c_1} \subset \mathcal{M}^N_{c_0,c_1}$, for all $N \geq 1$. Indeed, if $|o^{N+1}_{\mathbf{s}}(0)| < R_e$ for some template $\mathbf{s}$ then, from the escape radius condition, it follows that $|o^N_{\mathbf{s}}(0)| < R_e$ as well, which implies that $\mathcal{M}^N_{c_0c_1}$ are nester around $\mathcal{M}_{c_0,c_1}$. Subsequently, the intersection $\bigcap_{N=1}^{\infty} \mathcal{M}^N_{c_0,c_1} \supset \mathcal{M}_{c_0,c_1}$. On the other hand, if $|o^N_{\mathbf{s}}(0)| < R_e$ for all $N \geq 1$, then $\mathbf{s} \in \mathcal{M}_{c_0,c_1}$. Hence $\bigcap_{N=1}^{\infty} \mathcal{M}^N_{c_0,c_1} \subset \mathcal{M}_{c_0,c_1}$. In conclusion: $\bigcap_{N=1}^{\infty} \mathcal{M}^N_{c_0,c_1} = \mathcal{M}_{c_0,c_1}$.

□

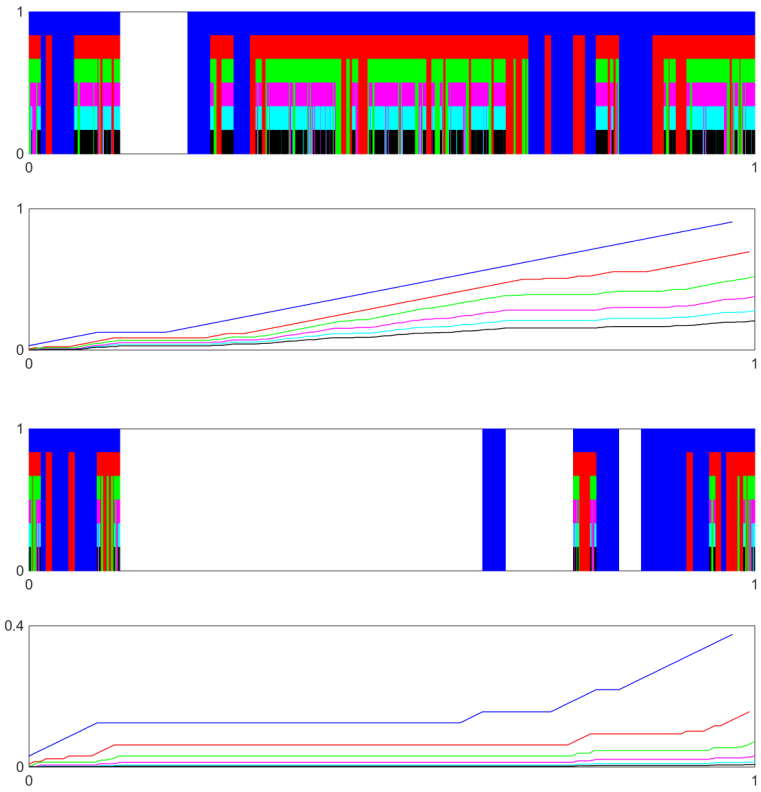

Figure 1: **N-rooted fixed-map Mandelbrot sets** *for two different map pairs* (c_0, c_1)*:* $c_0 = -0.117 - 0.76i$ *and* $c_1 = -0.62 - 0.62i$ *(***top***);* $c_0 = -0.75$ *and* $c_1 = -0.117 - 0.856i$ *(***bottom***). The top subplot of each panel shows sets* $\psi(\mathcal{M}^n_{c_0,c_1})$ *for different values of* N*, in different colors:* $N = 5$ *(blue),* $N = 7$ *(red),* $N = 9$ *(green),* $N = 11$ *(pink),* $N = 13$ *(cyan),* $N = 15$ *(black). To make it easier to simultaneously visualize these sets within the same copy of the unit interval, the sets were represented as blocks with hight decreasing from 1 to 1/3 for increasing* N*, layering out their structure for comparison (they are nested sets). The bottom subplot represents the accumulation map for each of the sets on top, in corresponding colors.*

Remark. Notice first that the intersection $\mathcal{M}_{c_0,c_1}$ is nonempty if either c_0 or c_1 are in the traditional Mandelbrot set, (since it will contain $\mathbf{s} = 00\ldots$, for the former, and $\mathbf{s} = 11\ldots$ for the latter), and it will be the empty set if both $|c_0| > 0$ and $|c_1| > 2$. The "size" of $\mathcal{M}_{c_0,c_1}$ for intermediate values of c_0 and c_1 will be further discussed in Section 3.

While the proof is straightforward, it is interesting to observe it at work for the representations of the sets on the unit interval, and compare with the illustrations of $\psi(\mathcal{M}^N_{c_0,c_1})$ and $\psi(\mathcal{M}_{c_0,c_1})$ in Figure 1. For a fixed N, there are 2^N possible N-roots $\langle \mathbf{s}^0 \rangle = 0\ldots00$, $\langle \mathbf{s}^1 \rangle = 0\ldots01$, on to $\langle \mathbf{s}^{2^N} \rangle = 1\ldots11$, whose images, together with the endpoint 1, form a partition of $[0, 1]$: $a^N_j = \psi(\mathbf{s}^j)$, for $j = 0, 2^N$, and $a^N_{2^N+1} = 1$. It is easy to see that $\psi(\mathcal{M}^N_{c_0,c_1})$ is a union of intervals $[a^N_j, a^N_{j+1})$. Similarly, $\psi(\mathcal{M}^{N+1}_{c_0,c_1})$ is a union of intervals $[a^{N+1}_j, a^{N+1}_{j+1})$ between points in the partition generated by all $N+1$-roots. Note that (a^{N+1}_j) is a finer partition than (a^N_j) – since it contains all points in (a^N_j) and the midpoints between those. Suppose now that an interval $[a^{N+1}_j, a^{N+1}_{j+1}) \subset \psi(\mathcal{M}^{N+1}_{c_0,c_1})$. This means that the last iterate of zero under the $N+1$-root $\langle \mathbf{s} \rangle = \psi^{-1}(a^{N+1}_j)$ is inside the escape disc. Subsequently, all the previous iterates under $\langle \mathbf{s} \rangle = s_1 s_2 \ldots s_{N+1}$ have to also be inside the escape disc. Consider the Nth root $\langle \mathbf{s}' \rangle = s_1 s_2 \ldots s_N$, and take $a^N_i = \langle \psi(\mathbf{s}') \rangle$. It follows that

$[a_j^{N+1}, a_{j+1}^{N+1}) \subset [a_i^N, a_{i+1}^N)$, in other words every interval in $\psi(\mathcal{M}_{c_0,c_1}^{N+1})$ is part of a subinterval in $\psi(\mathcal{M}_{c_0,c_1}^N)$. Figure 1 represents the sets $\psi(\mathcal{M}_{c_0,c_1}^N)$ in different colors for different values of N. In order to make the nested property more visible, we plotted them as 2-dimensional "combs" $\psi(\mathcal{M}_{c_0,c_1}^N) \times [0,h]$, where the hight h decreases with the value of N (so that one can observe a layering of nested combs of different colors as N increases).

We define the *accumulation map* of each "comb" (i.e., of each $\mathcal{M}_{c_0,c_1}^N$). Consider $\{0,1\}^N = \{\langle \mathbf{s}^1\rangle, \dots \langle \mathbf{s}^{2^N}\rangle\}$ the set of all N-roots, and their corresponding partition $a_j^N = \psi(\langle \mathbf{s}^j\rangle)$, for $j = 1, 2^N$, and $a_{2^N+1}^N = 1$. Then the accumulation map is given by:

$$\phi_{c_0,c_1}^N \colon [0,1] \to [0,1]$$

$$\phi_{c_0,c_1}^N(t) = \begin{cases} 0, \text{ at } t = 0 \\ \phi(a_j^N) \text{ on } [a_j^N, a_{j+1}^N], \text{ if } \langle \mathbf{s}^j\rangle \notin \mathcal{M}_{c_0,c_1}^N \\ \phi(a_j^N) + t - a_j^N \text{ on } [a_j^N, a_{j+1}^N], \text{ if } \langle \mathbf{s}^j\rangle \in \mathcal{M}_{c_0,c_1}^N \end{cases}$$

In other words, the map starts at $\phi(0) = 0$, increases by $1/2^N$ on each interval which is part of of comb, and remains constant on each interval which is not in the comb. Since the sets $\psi(\mathcal{M}_{c_0,c_1}^N)$ are nested, and the corresponding partition (a_j^N) becomes finer with increasing N, it follows that the accumulation map gets lower as N increases. The bottom subplots in Figure 1 show, for two different fixed pairs (c_0, c_1) in the two separate panels, a few instances of ϕ_{c_0,c_1}^N, for values of N for which the corresponding $\psi(\mathcal{M}_{c_0,c_1}^N)$ combs are plotted in the top subplots.

Consider now the point-wise limit of $\phi_{c_0,c_1} = \lim_{N\to\infty} \phi_{c_0,c_1}^N$. This is also a positive, monotonely increasing map of the interval, which we will call the accumulation map of $\mathcal{M}_{c_0,c_1}$. For the rest of the section, we will observe the topological structure of $\mathcal{M}_{c_0,c_1}$ for different pairs (c_0, c_1), by means of looking at the structure of the corresponding accumulation map ϕ_{c_0,c_1}, which we will prove to be a devil's straircase.

Notice that the structure of the staircase is specific to the order put on templates (via the map ψ). Its maximum value (which for this particular order of templates occurs at the end) is, however, order-independent. We will call this value the *full template value* of the pair (c_0, c_1), the limit of the *full N-root values* of (c_0, c_1): $\phi_{c_0,c_1}(1) = \lim_{N\to\infty} \phi_{c_0,c_1}^N(1)$. The value represents the likelihood for a random template $\in \{0,1\}^\infty$ to deliver a bounded critical orbit $o_{\mathbf{s}}(0)$ under the given functions f_{c_0} and f_{c_1}.

Definition 2.6. *We will say that the pair (c_0, c_1) is N-well behaved if the corresponding full N-root value $\phi_{c_0,c_1}^N(1) = 1$. We will say that the pair is infinitely well behaved if the full template value $\phi_{c_0,c_1}(1) = 1$.*

Remark. In other words, a pair is N-well behaved if the N iterates of the critical point remains inside the escape disc for *all* N-roots, under the given functions f_{c_0} and f_{c_1}. A pair is infinitely well behaved if it is N-well behaved for all N. This is equivalent to the critical orbit being bounded when iterating the given maps f_{c_0} and f_{c_1}, for almost all templates (seen as numbers on the unit interval, with the Lebesgue probability measure).

One interesting direction would be to analyze the topological structure of the graph of the accumulation map. In particular, we can investigate the frequency of plateaus of different lengths; for "devil's staircase" type graphs, this dependence follows a power law. In Figure 2, we represent this dependence for the same (c_0, c_1) parameter pairs for which the accumulation maps are shown in Figure 1. For a fixed N, we consider all possible plateau lengths $1 \le l \le 2^N$. For each l, we denote

by $s(l)$ the number of all plateaux with length l. In the two figure panels, we represent $\log(s+1)$ versus $log(l)$ (one was added to s in order to avoid getting an undefined value for lengths which are not represented). While the value of N used for both plots is $N = 20$ (making it perhaps too small to extrapolate to behavior as $N \to \infty$), the plots are reminiscent of log-log linear behavior, suggesting the possibility of a power law dependence in the limit of $N \to \infty$.

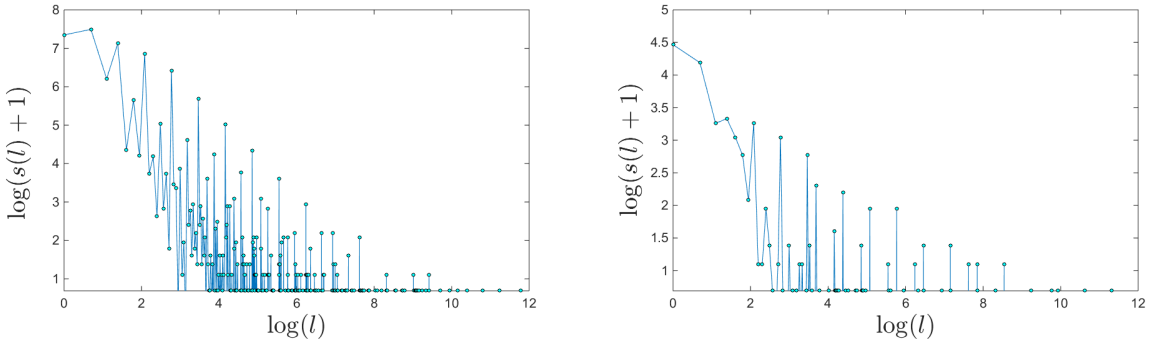

Figure 2: **Log-log representation of the distribution of plateau lengths** *for* $N = 20$ *and parameters* $c_0 = -0.117 - 0.76i$ *and* $c_1 = -0.62 - 0.62i$ *(***left***);* $c_0 = -0.75$ *and* $c_1 = -0.117 - 0.856i$ *(***right***).*

Another direction of potential interest is to study the one-dimensional topological structure of the fixed-map Mandelbrot set as the parameters c_0 and c_1 are begin varied. While this is clearly a potential (and probably more difficult) course, here we propose to first examine an easier dependence: that of the value $\varphi_{c_0,c_1}(1)$ on the complex parameter pair (c_0, c_1).

3 Hybrid, super-hybrid and mega-hybrid Mandelbrot sets

Fix now $c_0 \in \mathbb{C}$. With our new notation, and the escape radius restriction, we will look at the hybrid Mandelbrot set corresponding to c_0 as:

$$\mathcal{M}_{\mathbf{c_0}} = \{(c_1, b) \in \mathbb{D}(R_e) \times [0,1], \text{ with } b = \phi_{c_0,c_1}(1)\}$$

As before, one can also define root hybrid sets:

$$\mathcal{M}^N_{c_0} = \{(c_1, b) \in \mathbb{D}(R_e) \times [0,1], \text{ with } b = \phi^N_{c_0,c_1}(1)\}$$

Figure 3a illustrates the root hybrid set for $c_0 = 0$, for a root length of $N = 20$, with the value b corresponding to each c_1 represented as a color from blue to dark red. Recall that, for $c_0 = 0$, the critical orbit will always be bounded under the template with all entries zero. With this color map, blue region represent values of c_1 for which $\langle \mathbf{s} \rangle^0 = 0 \ldots 0$ is the only N-root that confines the critical orbit to the escape disc. The dark red central region represents the values of c_1 for which *all* N-roots confine the critical orbit to the escape disc. In other words, this is the region of c_1 for which the pair $(0, c_1)$ is N-well behaved.

Figure 3b illustrates this central part of the hybrid set by comparison with a truncated Mandelbrot set computed based on the same number N of iterates. Clearly, the former is a subset of the latter, property which remains true in the limit of $N \to \infty$:

$$\{c_1 \in \mathbb{D}(2) \text{ with } \phi_{0,c_1}(1) = 1\} \subset \mathcal{M} \subset \mathbb{D}(2)$$

where $\mathcal{M}$ is the traditional Mandelbrot set.

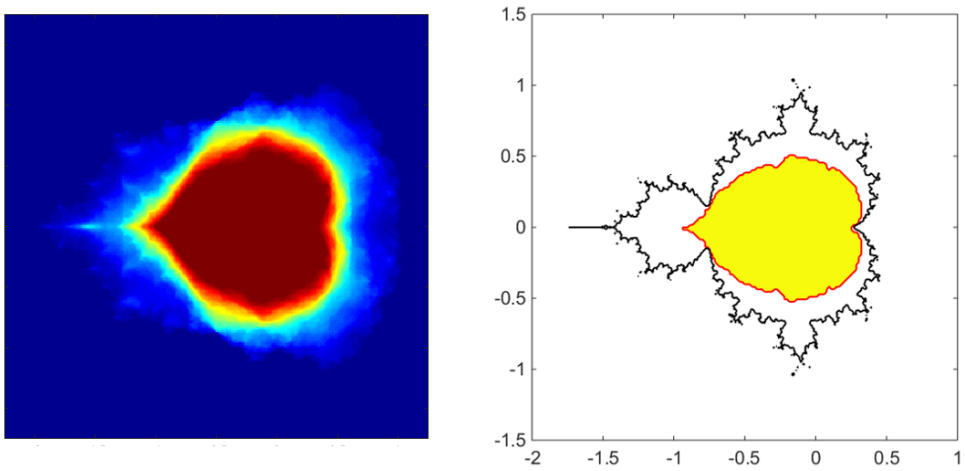

Figure 3: **Root hybrid Mandelbrot set $\mathcal{M}_0^N$ for $N = 20$. Left.** *Each pair (c_1, b) is represented as a pointc_1 in the complex plane with an associated color, coding the value of $b = \phi_{0,c_1}^{20}(1)$.* **Right.** *The shaded region corresponds to the N-well behaved pairs $\phi_{0,c_1}^N(1) = 1$ for $N = 20$, illustrated as a subset of a truncated representation of the traditional Mandelbrot set, computed for comparison also based on $N = 20$ iterations (the interior of the black curve).*

Theorem 3.1. *The set of infinitely well-behaved pairs $(0, c_1)$ contains the disc centered at the origin, of radius $1/4$.*

Proof. Consider $c_1 \in \mathbb{C}$, with $|c_1| < 1/4$. Then $\Delta = 1 - 4|c_1| > 0$, and one can define $d = \dfrac{1+\sqrt{\Delta}}{2} = \dfrac{1+\sqrt{1-4|c_1|}}{2} > 0$. Suppose now that $|z| < d$. It follows that

$$|z^2 + c_1| \quad \leq \quad |z|^2 + |c_1| \leq d^2 + |c_1| = \frac{1 + 2\sqrt{\Delta} + \Delta}{4} + |c_1| = \frac{1+\sqrt{\Delta}}{2} = d$$

Since $0 < d < 1$ it is also easy to see that, if $|z| < d$, then $|z^2| = |z|^2 < d^2 < d$. Subsequently: if $|z| < d$ then $|f_{c_{\mathbf{s}_n}}(z)| < d$, for all $n \geq 1$. Inductively, it follows that the orbit of $\xi_0 = 0 < d$ is completely contained in the disc of radius d around the origin, hence it is bounded. In conclusion: the critical orbit is bounded for all possible template iterations under the pair of maps $(0, c_1)$ with $|c_1| < 1/4$. In other words, the parameter disc centered at the origin and of radius $1/4$ is a subset of the set of infinitely well-behaved pairs $(0, c_1)$.

□

Based on our simulations, we conjecture the following for our set's topology:

Conjecture 3.2. *The set of infinitely well-behaved pairs $(0, c_1)$ is star-shaped connected.*

While the hybrid set for $c_0 = 0$ is perhaps the easiest to study and understand, one can consider hybrid sets for other values of c_0. Figure 4 illustrates the hybrid sets for a grid of c_0 complex values with $\mathrm{Re}(c_0) \in [-1.6, 1.6]$, and $\mathrm{Im}(c_0) \in [-0.4, 0.4]$. There are a few different ways in which one can organize this atlas of c_0-indexed hybrid sets. Below we describe two such ways, by defining two new higer-dimensional sets:

Definition 3.3. *The mega-hybrid Mandelbrot set is the set*

$$\mathcal{MM} = \{(c_0, b) \in \mathbb{D}(2) \times [0, 1], \ \textit{with } b = \max(\Pi_2(\mathcal{M}_{c_0}))\}$$

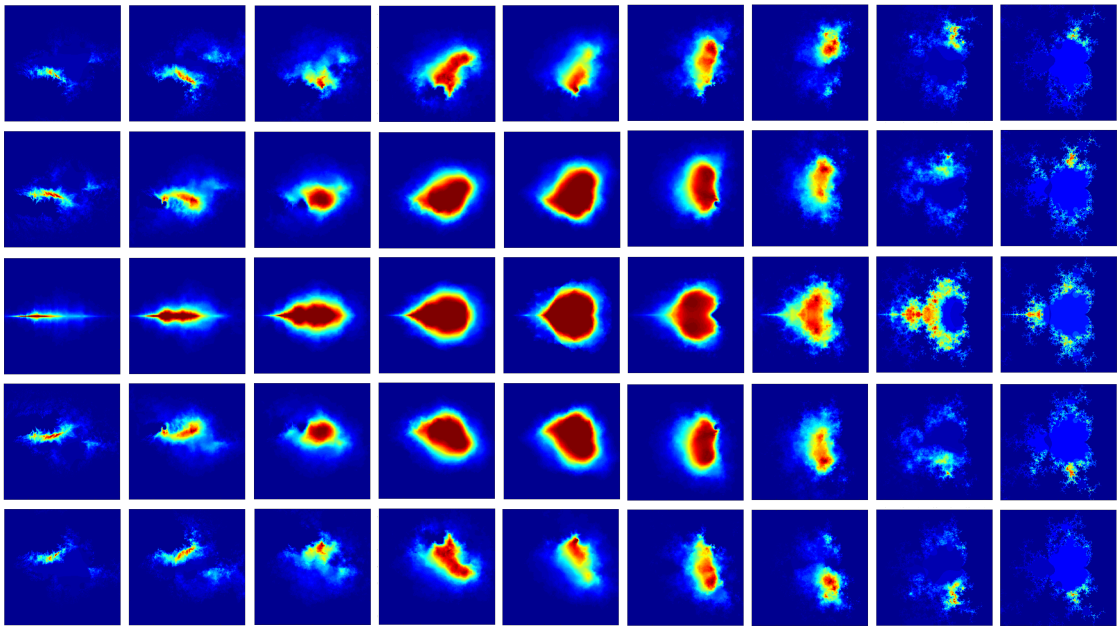

Figure 4: **Hybrid sets for a grid of c_0 values.** *The grid covers* $[-1.6, 1.6]$ *along the real axis and* $[-0.4, 0.4]$ *along the imaginary axis, with distance* 0.2 *in between sample values in both directions.*

where $\Pi_2(\mathcal{M}_{c_0})$ *designates the second component of the hybrid set* $\mathcal{M}_{c_0}$*. Similarly, one can define the* N*-root mega-hybrid Mandelbrot set as*

$$\mathcal{MM}^N = \{(c_0, b) \in \mathbb{D}(2) \times [0, 1], \ \textit{with } b = \max(\Pi_2(\mathcal{M}_{c_0}^N))\}$$

The mega-hybrid set assigns to every $c_0 \in \mathbb{D}(2)$ the largest value of $\phi_{c_0,c_1}(1)$ over all $c_1 \in \mathbb{D}(2)$. Similarly, one can assign to every c_0 the largest value of $\phi_{c_0,c_1}^N(1)$, and obtain the N-root mega-hybrid set – illustrated in Figure 5a for $N = 8$, with the colors representing, as before, different values of b.

One can consider the central (burgundy) plateau of $\mathcal{MM}^N$, representing all the values of $c_0 \in \mathbb{D}(2)$ for which there exists a $c_1 \in \mathbb{D}(2)$ such that (c_0, c_1) is N-well behaved. In Figure 5b, we illustrate the fact that the N-truncated Mandlebrot set is a subset of this central plateau, for all N. In the $N \to \infty$ limit, the Mandelbrot set is a subset of $c_0 \in \mathbb{D}(2)$ for which there is at least one c_1 with (c_0, c_1) infinitely well behaved.

Definition 3.4. *The super-hybrid Mandelbrot set is the set*

$$\mathcal{SM} = \{(c_0, c_1) \in \mathbb{D}^2(2), \ \textit{such that } \phi_{c_0,c_1}(1) = 1\}$$

and the N*-root super-hybrid Mandelbort set is*

$$\mathcal{SM}^N = \{(c_0, c_1) \in \mathbb{D}^2(2), \ \textit{such that } \phi_{c_0,c_1}^N(1) = 1\}$$

Remark. In other words, $\mathcal{SM}$ is the set of all infinitely well behaved parameter pairs in $\mathbb{D}(2)\times\mathbb{D}(2)$. Both $\mathcal{SM}$ and $\mathcal{SM}^N$ have complex dimension 2 (or real dimension 4). In Figure 6, we illustrate 3-dimensional slices of $\mathcal{SM}^N$.
While Figure 6 shows that not all 3D slices of $\mathcal{SM}^N$ are connected, we conjecture that

Conjecture 3.5. $\mathcal{SM}$ *is a connected set in* $\mathbb{C}^4$*.*

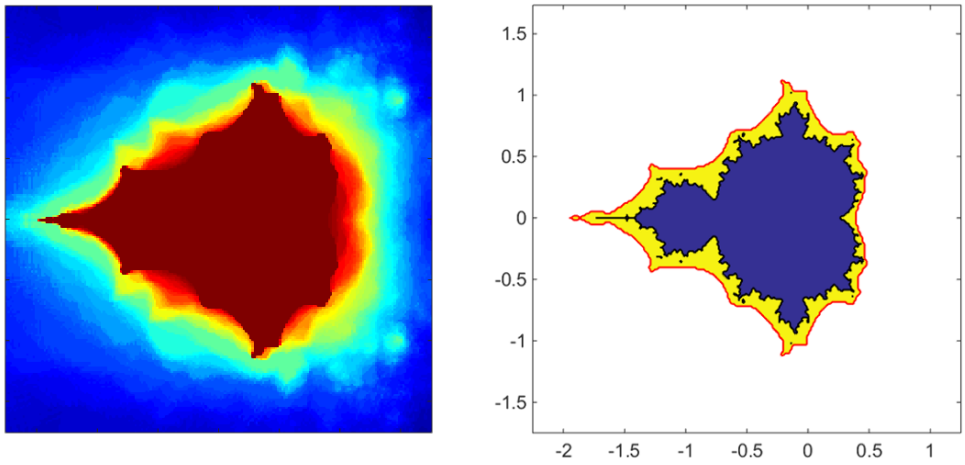

Figure 5: **N-root mega-hybrid Mandelbrod set,** *for $N = 8$. The colors represent values of b from zero (blue) to 2^N (dark red).*

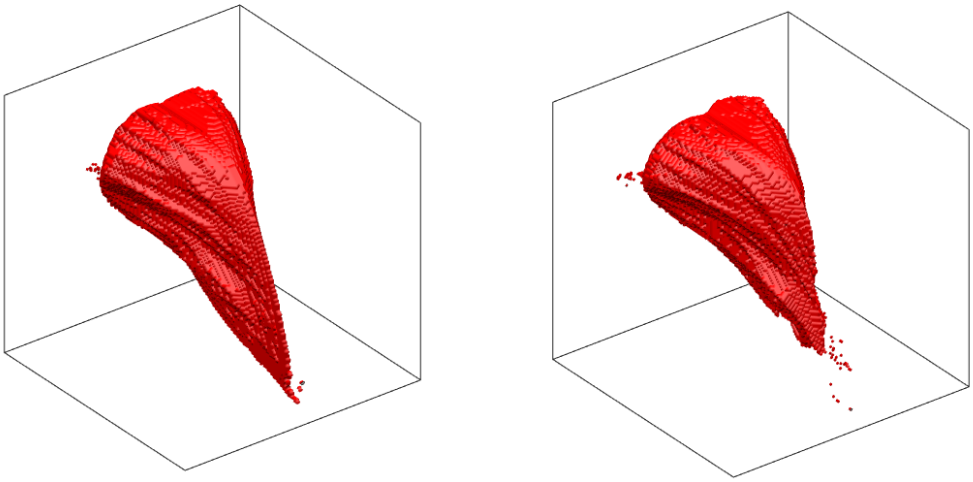

Figure 6: **Three-dimensional slices of the N-root super-hybrid set,** *for N=8.* **Left.** *Real $c_0 \in [-2, 1]$.* **Right.** *Complex $c_0 = Re(c_0) + 0.1i$, with $Re(c_0) \in [-2, 1]$.*

4 Discussion

In this paper, we expanded our investigations of the asymptotic dynamics of template iterations with new concepts and results. After introducing the *fixed template Mandelbrot* [13] in our previous work, in the current paper we concentrated on fixing the complex parameter pair (c_0, c_1), and understanding the topology of the *fixed-map* Mandelbrot set as a subset of the template space $\{0, 1\}^\infty$. We then defined *hybrid* sets which, for a fixed c_0 classify the values of c_1 based on how likely it is for a random template to produce a bounded critical orbit $o_{\mathbf{s}}(0)$.

The hybrid sets we define have a less complex geometric structure than the traditional Mandelbrot set (they do not have fractal behavior). This is not too surprising: the phenomenon of cooperation between generating maps has been already proposed by Sumi [14] as a contributor to decreasing the chaos in the overall system. However, this phenomenon was only described in the

context of averaged behavior over all initial conditions. Our numerical result seems to support a similar effect of randomness "smoothing out the chaotic structure" along the boundary of the Mandelbrot set. A better understanding of the latter, as well as a possible relationship between these two phenomena may become clearer with a more rigorous investigation of the topology of template Mandelbrot slices.

Our line of study includes understanding and interpreting the importance of this type of results in the context of models from natural sciences. One potential view, proposed by the authors in their previous joint work, is to interpret iterated orbits as describing the temporal evolution of an evolving system (e.g., copying and proofreading DNA sequences, or updating steps in a learning algorithm). Along these lines, an initial condition which escapes to ∞ under iterations may represent a feature of the system which becomes in time unsustainable, while an initial condition which is attracted to a simple periodic orbit may represent a feature which is too simple to be relevant or efficient for the system. Then the points on the boundary between these two behaviors (i.e., the Julia set) may be viewed as the set of optimal features, allowing the system to operate in a dynamic regime ideal for performing its complex function.

One can study how the "sustainable set of features" changes when introducing occasional or periodic errors into the iteration process. For example, one may be interested to understand for what types of errors the Julia set is disconnected, since that will indicate that the system may exhibit optimal function starting from more than one connected locus of initial conditions. In the traditional theory (due to the Fatou-Julia theorem) the critical point 0 is an important reference point, since the behavior of its orbit is indicative of the respective Julia set topology (if 0 is in the Julia set, then the Julia set is connected).

In our current work, we study the asymptotic behavior of the critical point when an "erroneous" function f_{c_1} interferes into the iteration of a correct function f_{c_0}. One natural question to ask in this context is how far can the erroneous map c_1 stray from the given correct map c_0, so that we can be sure (with some probability p) what the critical orbit $o_{\mathbf{s}}(0)$ stays bounded when a random template $\mathbf{s}$ prescribes where the errors will hit in the iteration process. To address and illustrate this question, and to obtain our first analytic insights into the answer, we defined and studied hybrid Mandelbrot sets.

This study only a step in establishing significant questions that can be addressed, in understanding their connection (similarities and differences) to the classical theory of single map iterations, and in exploring potential applications. A lot of theoretical work remains to be done, possibly exploring a brand new set of questions in discrete dynamics, requiring new methods from non-autonomous iterations, and the corresponding extensions for the concepts of critical and periodic orbits.

Acknowledgements

The work on this project was supported by the SUNY New Paltz Research Scholarship and Creative Activities program.

References

[1] Bodil Branner and John H Hubbard. The iteration of cubic polynomials part ii: patterns and parapatterns. *Acta mathematica*, 169(1):229–325, 1992.

[2] Lennart Carleson and Theodore W Gamelin. *Complex dynamics*, volume 69. Springer Science & Business Media, 1993.

[3] Mark Comerford. Hyperbolic non-autonomous julia sets. *Ergodic Theory and Dynamical Systems*, 26(02):353–377, 2006.

[4] Mark Comerford and Todd Woodard. Preservation of external rays in non-autonomous iteration. *Journal of Difference Equations and Applications*, 19(4):585–604, 2013.

[5] Marius-F Danca, M Romera, and G Pastor. Alternated julia sets and connectivity properties. *International Journal of Bifurcation and Chaos*, 19(06):2123–2129, 2009.

[6] Robert L Devaney and Daniel M Look. A criterion for sierpinski curve julia sets. In *Topology Proceedings*, volume 30, pages 163–179, 2006.

[7] John Erik Fornæss and Nessim Sibony. Random iterations of rational functions. *Ergodic Theory and Dynamical Systems*, 11(04):687–708, 1991.

[8] Robert E Johnson, M Todd Washington, Satya Prakash, and Louise Prakash. Fidelity of human dna polymerase η. *Journal of Biological Chemistry*, 275(11):7447–7450, 2000.

[9] Gaston Julia. Memoire sur l'iteration des fonctions rationnelles. *Journal de mathématiques pures et appliquées*, pages 47–246, 1918.

[10] Fatou, P.: Sur les équations fonctionnelles. Bulletin de la Société Mathématique de France **47**, 161–271 (1919)

[11] L Pray. Dna replication and causes of mutation. *Nature education*, 1(1):214, 2008.

[12] WeiYuan Qiu and YongCheng Yin. Proof of the branner-hubbard conjecture on cantor julia sets. *Science in China Series A: Mathematics*, 52(1):45–65, 2009.

[13] Anca Rdulescu and Ariel Pignatelli. Symbolic template iterations of complex quadratic maps. *Nonlinear Dynamics*, pages 1–18, 2015.

[14] Hiroki Sumi. Random complex dynamics and semigroups of holomorphic maps. *Proceedings of the London Mathematical Society*, page pdq013, 2010.

[15] user147263. Mandelbrot sets and radius of convergence. Mathematics Stack Exchange. URL:http://math.stackexchange.com/q/890448 (version: 2014-12-19).